Reprinted from JOURNAL OF COLLOID AND INTERFACE SCIENCE, Volume 33, No. 2, June 1970
 Printed in U.S.A.

Inertial Impaction of Particles upon Rectangular Bodies

KENNETH E. NOLL AND MICHAEL J. PILAT

Department of Civil Engineering, University of Washington, Seattle, Washington 98105

Received June 2, 1969; accepted November 6, 1969

The inertial impaction theory of aerosol particles upon the upstream face of rectangular collectors is reviewed. Both the theoretically calculated and measured particle deposition concentrations across the rectangular face are variable for low values of the Stokes' number ($K < 5$) and are nearly constant for high values ($K > 10$). The particle collection efficiencies calculated for three potential flow models are compared with the experimental measurements. The effect of the various Reynolds' numbers (local particle, free-stream particle, and free-stream collector Reynolds numbers) on the particle collection efficiency is discussed. A unique technique for sampling and sizing atmospheric giant particles (diameter greater than 1 μ) is described.

I. INTRODUCTION

The inertial impaction of particles upon objects has significance in many applications including particle collection efficiencies of air-sampling and air-cleaning devices, the icing of aircraft, and the washout by rain of airborne dust. The collection of particles upon bodies (aerodynamic capture) may be caused by a number of mechanisms: inertial impaction, interception, Brownian diffusion, thermal diffusion, and electrostatic precipitation. Fortunately in some cases one mechanism predominates allowing simplifying assumptions to be made.

The first important investigations of inertial impaction were by Sell (1) and Albrecht (2). Sell studied velocity profiles experimentally and calculated particle trajectories around various shaped objects. Albrecht used potential-flow equations to calculate the collection efficiency of simple bodies. Since then inertial impaction studies have been focused mainly on three simple body geometries—cylinders, spheres, and rectangles. The theoretical particle collection efficiency for these body types have been provided by a number of investigators including Langmuir and Blodgett (3), Ranz and Wong (4), Wong, Ranz, and Johnstone (5), and Lewis and Brun (6), and have been summarized by Golovin and Putnam (7). Experimental determinations of particle collection efficiencies have been reported for cylinders and spheres but not for rectangles.

This paper considers the particle collection efficiency due to inertial impaction upon rectangular bodies of infinite extent in one direction (often called infinite strips or ribbons) and includes:

1) Calculations of particle trajectories and rectangular body total and local collection efficiencies in potential flow ($Re_t > 1000$).

2) Experimental determination of the total and local collection efficiencies of particles upon the upstream face of rectangular bodies.

3) Experimental measurement of the size distribution of particles collected on the upstream face of a rectangular collector.

This investigation was undertaken to evaluate a new rotary inertial impactor designed by Noll (8) to sample atmospheric giant particles (diameter greater than 1 μ). The atmospheric aerosol was used in the experimental evaluation of the rectangular collectors of the rotary inertial impactor. Although a laboratory-generated aerosol may have more uniform properties, the atmospheric aerosol proved sufficiently accu-

rate for determining the optimum performance range of the new impactor (Stokes' number larger than 10). This study presents the first experimental measurements of the total and local particle collection efficiencies of rectangular bodies under potential flow conditions. The particle collection efficiencies for three previously published potential flow models are reviewed and compared with the experimental results.

II. THEORY

Equation of Motion for Particle in Fluid Flowing around Object

A particle suspended in a flowing gas stream tends to move in a straight line because of its inertia. When the gas stream flows around a collecting body all the aerosol particles follow the gas streamlines until they begin to curve around the body. The larger particles have sufficient momentum to continue their motion toward the collector and impact upon its surface. Smaller particles fail to reach the collector surface because of fluid resistance and insufficient momentum. The equation of motion in vector notation for a particle of mass m is:

$$m\, d\bar{u}/dt = -\bar{F}. \qquad [1]$$

If all external forces on the particle are neglected $\bar{F}$ is the drag force of the fluid on the particle and is given by:

$$\bar{F} = (C_d Re/243)\, \pi\mu(\bar{u} - \bar{v})\, d. \qquad [2]$$

If we assume the particles to be spherical and use a dimensionless form, the equation of motion in rectangular coordinates becomes:

$$\frac{48K}{C_d R_e}\frac{d^2x}{dt^2} + \frac{dx}{dt} - v_x = 0; \qquad [3]$$

$$\frac{48K}{C_d R_e}\frac{d^2y}{dt^2} + \frac{dy}{dt} - v_y = 0. \qquad [4]$$

For these equations the origin is located at the center of the front face of the collector, and the unit of distance is the diameter or width L of the collector. The dimensionless air velocity components v_x and v_y and the particle velocity components u_x and u_y are referred to the free-stream velocity v_0 as shown in Fig. 1. Time is expressed in terms of the dimensionless quantity $t = 2t_0v_0/L$. The unit of time is that time required to move a distance $1/2L$ at a velocity v_0. Here K is an inertial parameter known as the Stokes' number and is defined as:

$$K = \frac{\rho_p d^2 v_0}{18\mu L}. \qquad [5]$$

The Stokes' number is the ratio of the particle stop distance (distance particle will

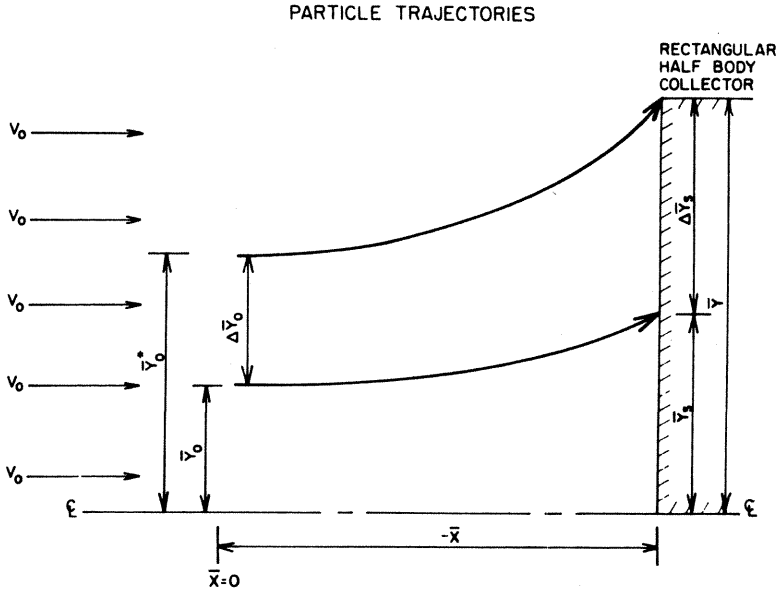

Fig. 1. Trajectories of particles approaching rectangular collector.

penetrate into a still fluid when given an inertial velocity u_0) to the collector half width.

There are three Reynolds' numbers involved in this system, the local particle Reynolds' number $Re = d(\bar{u} - \bar{v})\rho_f/\mu$, the free-stream Reynolds' number of the particle $Re_0 = dv_0\rho_f/\mu$, and the collector or target Reynolds' number $Re_t = Lv_0\rho_f/\mu$. It should be noted that these Reynolds' numbers are frequently used but not defined clearly in inertial impaction literature. The free-stream Reynolds' number Re_0 and the particle Reynolds number Re are related by:

$$Re = Re_0[v_x - u_x)^2 + (v_y - u_y)^2]^{1/2}. \quad [6]$$

An empirical equation reported by Langmuir and Blodgett (3) was used to calculate the drag coefficient C_d as a function of the particle Reynolds' number ($0 < Re < 10^5$).

$$\frac{C_dRe}{24} = 1 + 0.197Re^{0.63} + 2.6 \times 10^{-4}Re^{1.38}. \quad [7]$$

Another dimensionless parameter (frequently used as the Reynolds' number variable) is the modified target Reynolds' number ϕ:

$$\phi = \frac{Re_0^2}{K} = \frac{9\rho_f Re_t}{\rho_p}. \quad [8]$$

The particle collection efficiency and the Stokes number are usually related to ϕ. The main advantage claimed for using ϕ is that it is not a function of the particle diameter.

Fluid Flow Fields

A solution of the particle equations of motion, Eq. [3] and [4], requires information about the fluid flow field (v_x and v_y). For the region upstream of the collector, the fluid velocity flow field at high target Reynolds' number may be considered to be the same as potential flow (fluid is ideal, inviscid, irrotational, and incompressible). Three potential flow fields around a rectangular collector, which are shown in Fig. 2, are: (1) flow around a ribbon normal to the flow (3), (2) flow around a rectangular half body (6), and (3) flow in a corner of infinite extent (9).

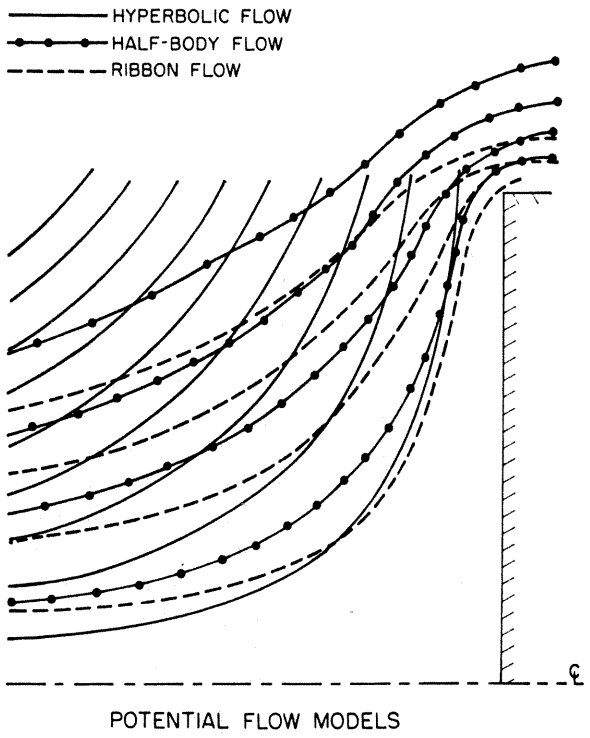

FIG. 2. Fluid streamlines for three potential flow fields.

The flow in a corner of infinite extent is the simplest flow pattern. The equations of the fluid streamlines are hyperbolas:

$$y_0 = -xy = \text{constant} \quad [9]$$

with the fluid velocity field for the region $0 > x > -1$ and $1 > y > 0$ given by:

$$v_x = -x; \quad [10]$$

$$v_y = y. \quad [11]$$

This flow pattern linearizes the particle equation of motion.

The fluid velocity components for potential flow around a ribbon normal to the flow are

$$v_x = \left[\frac{y^2(x^2 + y_0^2)^2}{x^2(x^2 + y_0^2)^2 + x^2(y^2 - y_0^2)^2}\right]^{1/2}; \quad [12]$$

$$v_y = \left[\frac{x^2(y^2 - y_0^2)^2}{y^2(x^2 + y_0^2)^2 + x^2(y^2 - y_0^2)^2}\right]^{1/2}. \quad [13]$$

These flow fields were used to provide the fluid velocities v_x and v_y for the equations of particle motion, Eq. [3] and [4]. The fluid velocity profile for flow around a rectangular half body was not used in the present calcu-

lations but is shown in Fig. 2 to provide a comparison of the three potential flow fields.

Efficiency of Particle Collection upon Object

Total Collection Efficiency

The total particulate collection efficiency of an object can be defined as the ratio of the number of particles striking the object to the number of particles which would strike the object if the particle trajectories were all straight lines, parallel to the direction of the undisturbed fluid flow. The solutions of the equation of motion for the particles at various magnitudes of K and Re result in a series of trajectories originating at y_0 (trajectory starting ordinate) and which either intersect the collector surface or pass around it. One of these trajectories, which originates at y_0^* and is tangent to the collector edge, determines the collection efficiency. Such a limiting trajectory is illustrated in Fig. 1. If it is assumed that the particles are uniformly distributed in the fluid, are of diameter negligible compared to that of the collector width, and stick upon impaction, the total collection efficiency E upon the upstream face of a rectangular body is the ratio of the limiting trajectory ordinate to the body half width.

$$E = \frac{2y_0^*}{L}. \qquad [14]$$

Local Collection Efficiency

The number distribution of monodisperse particles collected across the face of a rectangular object has been calculated by Lewis and Brun (6) using potential flow around a half body. They reported that the local collection efficiency at low Stokes' number varied across the collector face with the maximum efficiency occurring at the collector edge. At high Stokes' number the local collection efficiency was uniform across the collector face. However, too few trajectories were reported to determine accurately the shape of the local collection efficiency profile. To clarify this situation the local particle collection efficiency across the upstream face of a rectangular object was calculated for the other two potential flow patterns, flow around a ribbon and flow in a corner of infinite extent.

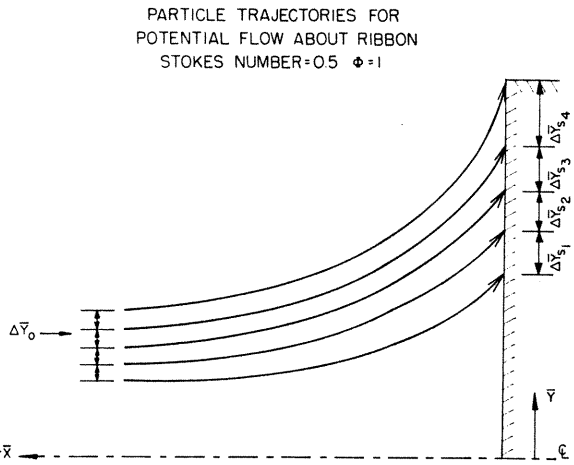

FIG. 3. Particle trajectories showing that the nonlinear equation of particle motion produces variations in Δy_s for equal Δy_0 (flow around a ribbon).

The local particle collection efficiency B can be approximated by

$$B = \frac{\Delta y_0}{\Delta y_s}, \qquad [15]$$

where y_s is the ordinate at the collector face surface for a certain y_0 (ordinate at the trajectory starting point). When a collector moves through a uniformly distributed aerosol, the particles between any two trajectories with starting ordinates y_{0_1} and y_{0_2} will arrive at the collector surface between the same two trajectories' terminal ordinates, y_{s_1} and y_{s_2} as shown in Fig. 3. The quantity of aerosol between the trajectories represented by $\Delta y_0 = y_{0_2} - y_{0_1}$ is equal to the quantity of aerosol impinging upon the collector between the interval $\Delta y_s = y_{s_2} - y_{s_1}$ (the quantity of aerosol between adjacent particle trajectories remains constant).

III. THEORETICAL RESULTS

Solution to Equation of Motion

The equations of particle motion were solved using an analog computer to determine the particle trajectories with respect to the collector face. Particle trajectories were calculated for various magnitudes of K, Re_0, and y_0. The general calculation procedure included:

1) Establishment of the fluid velocity flow field upstream of the collector (provide v_x and v_y).

2) Selection of the magnitudes of K and Re_0.

3) Selection of the magnitude of y_0.

4) Calculation of the variable $C_dRe/24$ using Eq. [7] (used variable diode function generator, VDFG).

5) Performance of the calculations to determine the particle trajectories including the limiting trajectory y_0*.

The particle trajectories which were obtained by this procedure were used to determine the total collection efficiency of the rectangular collector and the local particle collection pattern across the collector face. A comparison of the collection efficiencies for various fluid flow models was also obtained.

Total Collection Efficiency

The total particle collection efficiency of the upstream face of a rectangular object as a function of the Stokes' number is shown in Fig. 4. The data for the half-body flow curve were reported by Lewis and Brun (6). Note that the curve for the hyperbolic fluid flow field does not have the typical "S" shape of the other curves obtained using the nonlinear equations of motion.

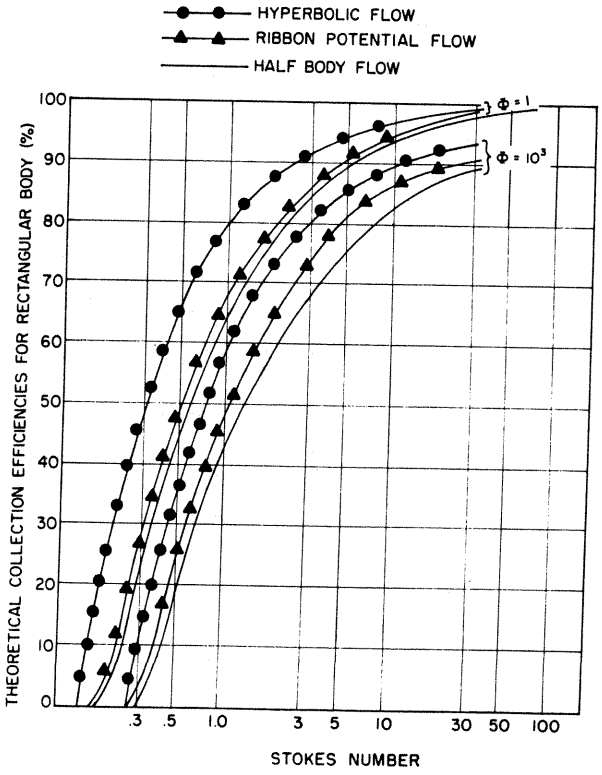

Fig. 4. Calculated total particle collection efficiencies as a function of Stokes' number for three potential flow fields.

Local Collection Efficiency

The local particle collection efficiencies for flow around a ribbon at various Stokes' numbers is presented in Fig. 5. At high magnitudes of K ($K > 10$) the local collection efficiency B approaches unity. At low magnitudes of K ($K < 0.1$) B approaches zero. The greatest change of the local collection efficiency with distance across the collector face occurs at Stokes' numbers near one. The particles with Stokes' numbers of this magnitude are most unevenly distributed with the maximum particle concentration occurring near the collector edge and the minimum concentration near the collector center.

The hyperbolic fluid flow field described by Eqs. [10] and [11] provides a local particle collection efficiency which is uniform across the collector face at all magnitudes of the Stokes' number. This occurs because the equation of motion is linear for this flow field. The particle trajectories computed for flow around a ribbon (Eqs. [12] and [13]) are shown in Fig. 3. These trajectories are not parallel and thus the local particle collection efficiency varies across the face.

IV. Measurement of Collection Efficiency

Type of Aerosol

Previous experimental measurements of the particulate collection efficiency on cylinders and spheres have involved the use of either a monodisperse aerosol or a liquid polydisperse aerosol. Gregory (10), using Lycopodium spores with a diameter very near 32 mμ, determined the collection efficiencies of particles upon various-sized glass cylinders at five air velocities. Wong *et al.* (5) generated a nearly uniform sulfuric acid aerosol for impaction upon cylinders. The quantity of particles collected on the cylinders was measured with a precision conductivity bridge.

The atmospheric aerosol was used in this research project. For a qualitative comparison of the experimental and theoretical particle collection efficiencies it was desirable that the aerosol size distribution be con-

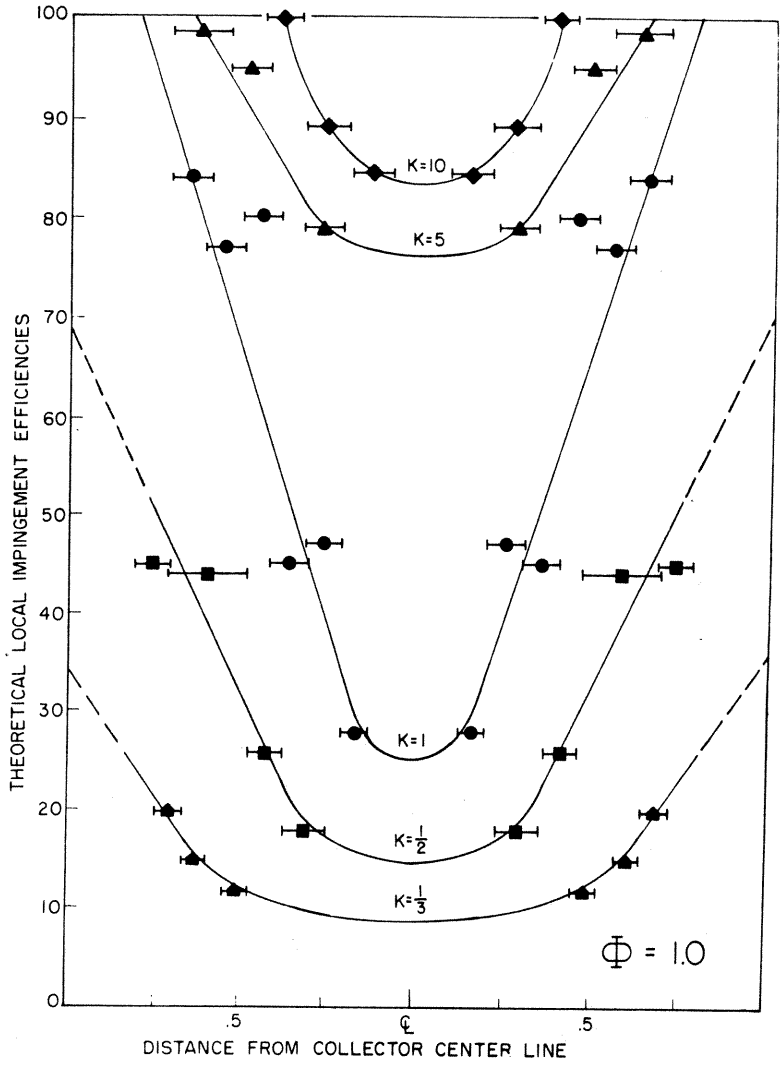

FIG. 5. Variation in the calculated local particle collection efficiency as a function of distance from the collector center line and of Stokes' number.

tinuous (that the particle concentration between radius r and $r + dr$ be a continuous function of r). This condition occurs with the atmospheric aerosol as reported by Junge (11), Clark and Whitby (12), Pueschel and Noll (13), and Cataneo and Stout (14). However, the rotary inertial impactor can be used to sample aerosols of discontinuous as well as continuous size distributions.

IMPACTOR DESIGN

Atmospheric aerosol particles were collected on various-sized rectangular collectors moving at different velocities. The collectors effectively separated the atmospheric aerosol into different size ranges. A Stokes' number of 10 was selected as the design criteria for the stages. As shown in Fig. 4 this Stokes' number corresponds to a collection efficiency of between 85% and 100% depending on the target Reynolds' number and the flow field. With a Stokes' number of 10 and a particle density of 2 grams/cc Eq. [5] can be transformed into the following sampling stage design equation for the minimum particle diameter d collected with 85% or greater efficiency:

$$d = (HL/v_0)^{1/2}, \qquad [16]$$

where H is a constant equal to 0.0162 when cgs units are used.

A 16-stage impactor with rectangular collectors of various widths, illustrated in Fig. 6, was used in this study. A stage consists of a

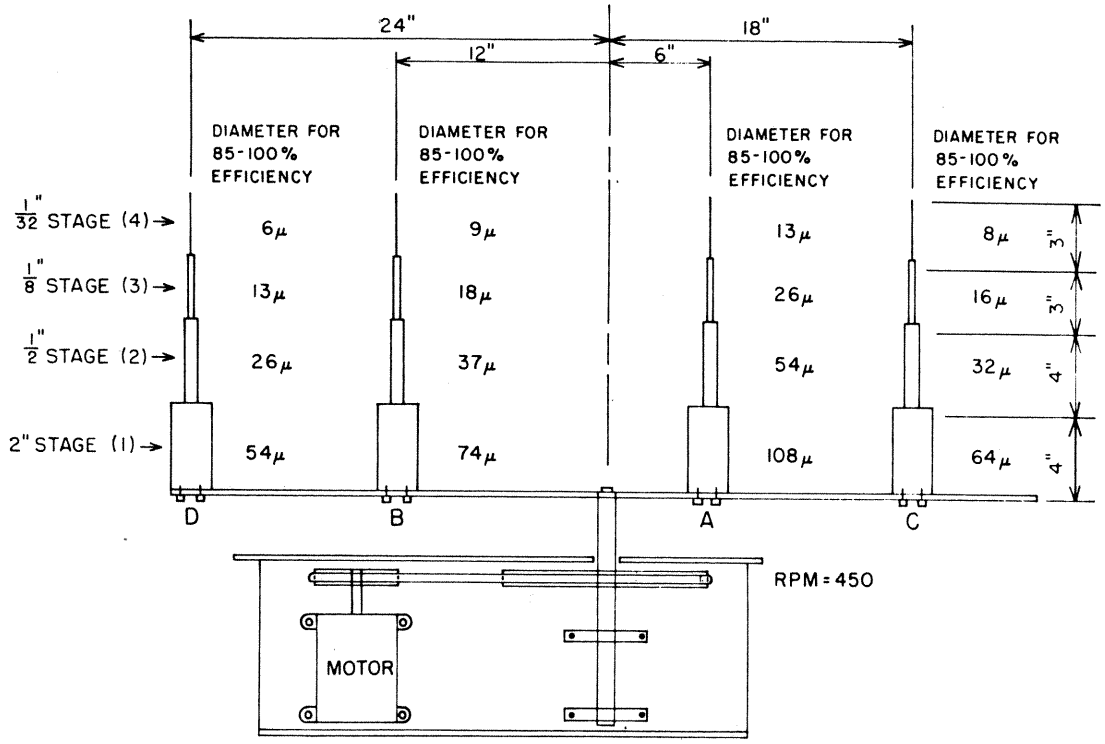

FIG. 6. Atmospheric giant particle inertial impactor.

collector of a certain width operating at a given air velocity. Various combinations of collector widths and air velocities (rotor-arm lengths) provided equivalent Stokes' numbers on various stages (designed this way for cross-checking purposes). Each collector is four times as wide as the next smaller stage at the same air velocity position (L of $\frac{1}{32}$ in., $\frac{1}{8}$ in., $\frac{1}{2}$ in., and 2 in.) so as to provide a factor of two charge in the minimum particle diameter collected as defined by the stage design criteria, Eq. [16]. The rotor arm was designed to operate at 450 rpm. The four collector stations are located at 6, 12, 18, and 24 in. from the rotor-arm axis thus providing air velocities of 17, 34, 52, and 68 mph. With a wind speed greater than 3 mph the air motion is sufficient to provide fresh air to the impactors and thus resampling of the air is prevented. The minimum particle diameter for 85% or greater collection efficiency for each stage is shown in Fig. 6.

EXPERIMENTAL PROCEDURE

Samples of the atmospheric aerosol were collected by exposing the moving rectangular collectors to the outside air for time periods ranging from 15 min to 2 hours. The collector surfaces were coated with Vaseline to ensure retention of the impacted particles. The collected particles were sized and counted by visual methods with a Zeiss microscope–television camera–TV monitor arrangement. Overhead illumination was used thus allowing the collector face to be viewed directly without any cover glass between the collected particles and the microscope objectives lens.

EXPERIMENTAL RESULTS

Local Particle Collection Efficiency

The concentration of particles on the collector face was determined by counting and sizing the impacted particle at various distances from the collector center line. A typical variation in the particle concentration across the collector faces is shown in Fig. 7. As was predicted theoretically, at low Stokes' number the particle concentration was unevely distributed with a low concentration near the collector center and a maximum near the edge. The mimimum collec-

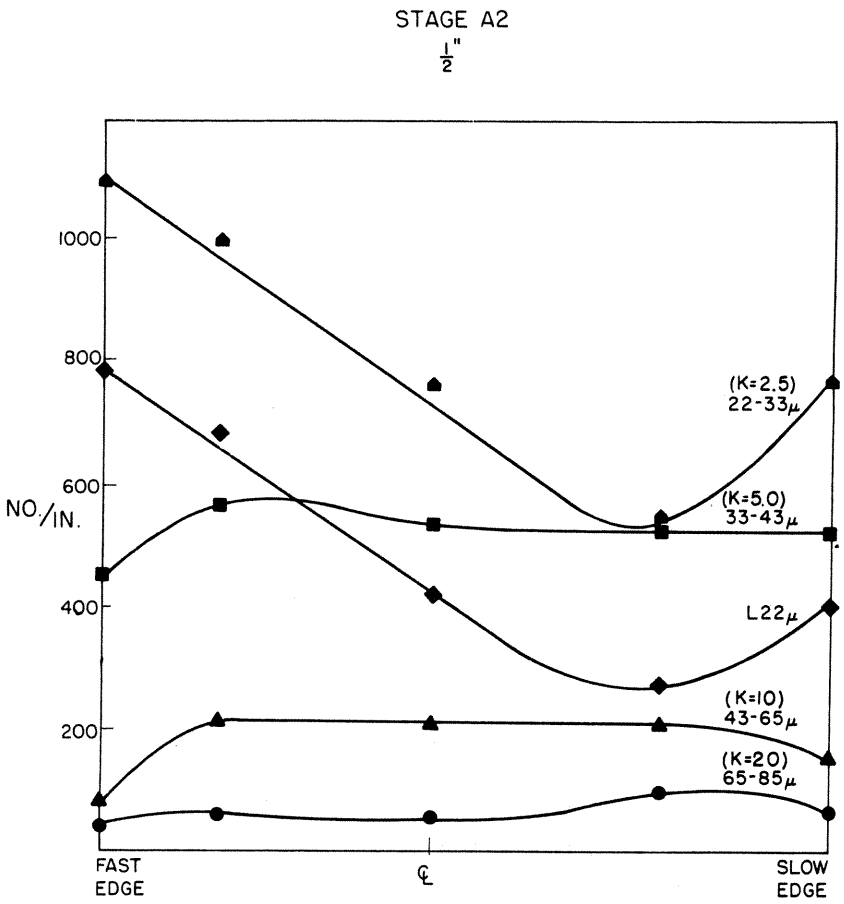

FIG. 7. Measured variations of the particle concentration on the collector face as a function of Stokes' number and distance from the collector center line.

tion efficiency, which should occur at the collector center line as shown in Fig. 5, is displaced in Fig. 7 because of the air velocity difference across the collector face (caused by the outside edge of the collector moving faster than the inside edge). The air velocity difference across the collector face decreases with the decrease in collector width and with the increase in the distance of the collector from the center of rotation. The variation across the face of the local particle collection efficiency decreased with increasing particle size. The particles of interest on each stage ($K > 10$) were nearly uniformly distributed.

Total Particle Collection Efficiency

To determine the total particle collection efficiency of an impactor two quantities should be measured: (1) the concentration of aerosol particles approaching the impactor, and (2) the number of particles collected on the impactor per unit time. As there are no other instruments to accurately sample giant particles in the atmosphere the first quantity mentioned above was not measured. However, it is possible to estimate the total particle collection efficiency by three approaches.

First the theoretical analyses of inertial impaction predict that at high Stokes' numbers ($K > 10$) a nearly uniform particle concentration will exist across the collector face. Thus the particle sizes which are experimentally determined to be uniformly distributed across the collector surface will have high Stokes' numbers ($K > 10$) and high collection efficiency (greater than 85%).

Secondly a comparison of the collection efficiencies of the various stages can be made by plotting the aerosol concentration versus the particle size, as shown in Fig. 8. It can be seen in this figure that the concentrations of the same-sized particles collected on different

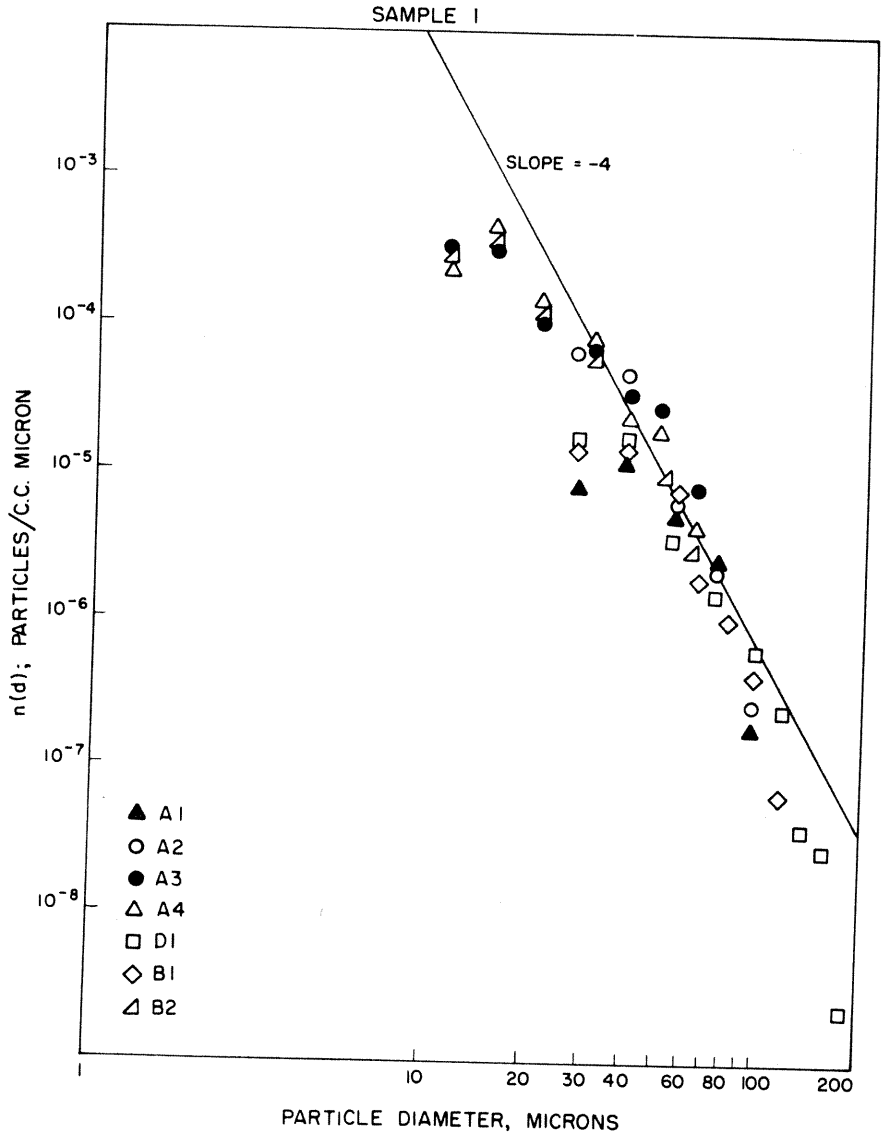

FIG. 8. Size distribution of giant particles in the atmospheric determined by combining data from a number of collector stages.

stages are nearly the same, indicating equal collection efficiencies. The line was drawn through those particle concentration points determined from particles uniformly distributed across the collector face. Also the particle concentration is continuous and has a slope of -4, agreeing with the atmospheric aerosol size distribution theory reported by Junge (15). These features imply equivalent collection efficiencies (interpreted to be near 100%) on different stages.

Thirdly, the particles which were unevenly distributed across the collector face provide aerosol concentrations which were less than expected (were less than concentrations of uniformly distributed particles). The experimental collection efficiencies for these unevenly distributed particles were determined by measuring the magnitude of the deviation from the size distribution line in Fig. 8. The experimental collection efficiencies shown in Fig. 9 show a qualitative comparison with the theoretical efficiencies presented in Fig. 4.

In Fig. 9 the decrease in particle collection efficiency at constant Stokes' number and collector width (curves for stages *A1*, *B1*, and *D1*) with increasing target Reynolds' number (increasing ϕ values) is due to increased drag on the particle. The particle

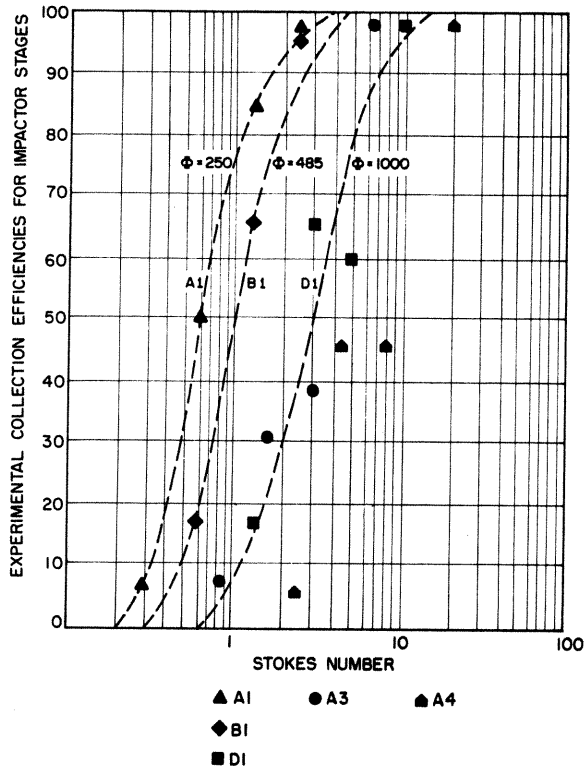

FIG. 9. Measured total particle collection efficiency for various collector stages as a function of Stokes' number.

drag coefficient C_d, described empirically by Eq. [7], is a direct function of the local Reynolds' number of the particle (Re). Examination of the particle equations of motion, Eqs [3] and [4], shows that increasing the drag coefficient C_d essentially reduces the calculated collection efficiency. The theoretically predicted (Fig. 4) and the experimentally measured (Fig. 9) decreases in particle collection efficiency are in qualitative agreement.

In Fig. 9 the displacement of experimental points for stages *A3* and *A4* is probably caused by the air flow conditions not being potential for these stages. The target Reynolds' numbers of stages *A3* and *A4* are 1800 ($\phi = 15$) and 450 ($\phi = 5$), respectively. Green and Lane (16) reported that the assumption of potential flow conditions requires a target Reynolds' number of at least 1000. For flow at target Reynolds' numbers less than 1000 (transition and laminar flow regions) the particle collection efficiencies are less than for potential flow. Stages *A1*, *B1*, and *D1* have target Reynolds' numbers of 29,000 ($\phi = 250$), 57,000 ($\phi = 485$), and 120,000 ($\phi = 1000$), respectively, and have measured collection efficiencies which agree with potential flow theory.

V. SUMMARY

This investigation has summarized the theory of inertial impaction on rectangular bodies. The effect on the collection efficiency of the various Reynolds' numbers used in the literature has been clarified. The target Reynolds' number is important to the assumption of potential flow and the local Reynolds' number is significant to the fluid drag on the particles.

The theoretical and actual particle distribution patterns across the face of a rectangular collector were compared. Both showed that the particle concentration was variable for low values of the Stokes' number ($K < 5$) but was nearly constant for high values ($K > 10$).

The over-all collection efficiency was obtained with three different potential flow models and compared qualitatively with experimentally determined efficiencies. The experimental efficiencies were obtained by comparing the concentration of particles collected on rectangular collectors of different widths mounted on a rotating blade and exposed to atmospheric particles. A continuous particle-size distribution resulted for these particles. An equivalent concentration was obtained for the same size particle collected on collectors of different widths moving at different velocities.

ACKNOWLEDGMENTS

This research was supported by USPHS National Air Pollution Control Administration Special Fellowship No. 1 F3 AP 38, 939-01 and Training Grant AP-29. The assistance of Dr. R. H. Bogan and M. S. Merrill with the analog computations and the discussions with Dr. C. A. Sleicher and Dr. R. J. Charlson are gratefully acknowledged.

NOMENCLATURE

B	—Local impingement efficiency.
C_d	—Coefficient of drag.
d	—Particle diameter.
E	—Over-all collection efficiency.
F	—Resistance of fluid.

H —Constant equal to 0.0162.
K —Stokes' number—particle inertial parameter.
L —Width of rectangular collector.
m —Mass of particle.
Re —Local Reynolds' number with respect to particle.
Re_0 —Free-stream Reynolds' number with respect to particle.
Re_t —Reynolds' number with respect to target or collector.
t —Dimensionless time function, $2v_0t/L$.
v_0 —Free-stream fluid velocity.
v_x , v_y—Dimensionless local air velocity components—v_x/v_0 , v_y/v_0.
u —Velocity of particle.
u_x,u_y —Particle velocity components.
x —Dimensionless distance from collector center line, $2y/L$.
y_0 —Trajectory starting ordinate.
y_0* —Trajectory starting ordinate which is tangent to edge of collector.
y_s —Trajectory point of impingement on collector face.

GREEK SYMBOLS

ρ_f —Density of fluid.
ρp —Density of particle.
μ —Viscosity of fluid
ϕ —Dimensionless parameter $= Re_0^2/K = 9(\rho_f/\rho_a)Re_t$.

REFERENCES

1. Sell, W., "Dust Precipitation on Simple Bodies and in Air Filters," *Forsch. Gebiete Ingenieurw.* **2,** 347. *In Univ. Illinois Tech. Rept.* **3** (1951) (Translated by P. J. Domoter).
2. Albrecht, F., "Theoretical Investigations of Dust Deposition from Flowing Air and Its Application to the Theory of the Dust Filter," *Physik. Z.* **32,** 48 (1931). *Univ. Illinois Tech. Rept.* **3** (1951) (Translated by P. J. Domoter).
3. Langmuir, I., and Blodgett, K. B., "Mathematical Investigation of Water Droplet Trajectories," General Electric report RL 225 Ad 64354 (1945).
4. Ranz, W. E., and Wong, J. B., "Impaction of Dust and Smoke Particles," *Ind. Eng. Chem.* **44,** 1371 (1952).
5. Wong, J. B., Ranz, W. E., and Johnstone, H. F., "Inertial Impaction of Aerosol Particles on Cylinders," *J. Appl. Phys.* **26,** 244 (1955).
6. Lewis, W., and Brun, R. J., "Impingement of Water Droplets on a Rectangular Half Body in a Two-Dimensional Incompressible Flow Field," *NASA Tech. Note* **TN 3658** (1956).
7. Golovin, M. N., and Putman, A. A., "Inertial Impaction on Single Elements," *Ind. Eng. Chem. Fundamentals* **1,** 264 (1962).
8. Noll, K. E., "A Rotary Inertial Impactor for Sampling Giant Particles in the Atmosphere," *Atmospheric Environment* **4,** 9 (1970).
9. Ranz, W. E., "The Impaction of Aerosol Particles on Cylinders and Spherical Collectors," *Univ. Illinois Eng. Expt. Sta. Tech. Rept.* **3** (1951).
10. Gregory, P. H., "Deposition of Air-borne Lycopodium Spores on Cylinders." *Ann. Appl. Biol.* **38,** 357 (1951).
11. Junge, C. E., "The Size Distribution and Aging of Natural Aerosol as Determined from Electrical and Optical Data on the Atmosphere," *J. Meteorol.* **12,** 13 (1955).
12. Clark, W. E., and Whitby, K. T., "Concentration and Size Distribution Measurements of Atmospheric Aerosols and a Test of the Theory of Self-Preserving Size Distribution," *J. Atmospheric Sci.* **24,** 677 (1967).
13. Pueschel, R. F., and Noll, K. E., "Visibility and Aerosol Size Frequency Distribution," *J. Appl. Meteorol.* **6,** 1045 (1967).
14. Cataneo, R., and Stout, G. E., "Raindrop-Size Distributions in Humid Continental Climates, and Associated Rainfall Rate-Radar Reflectivity Relationships," *J. Appl. Meteorol.* **7,** 901 (1968).